National Conference with International Participation
ENGINEERING MECHANICS 2006
Svratka, Czech Republic, May 15 – 18, 2006
paper no. 288

SIMULATION OF AUTOGENOUS SHRINKAGE OF YOUNG CEMENT PASTES

V. Šmilauer, J. Litoš [1]

Summary: *Autogenous shrinkage presents a serious problem in modern concretes due to various admixtures and high water demand for hydration. Microscopic underpressure in the pore water exerts inner load to the microstructure, causing shrinkage and consequently creep. This behavior is simulated via FEM, where the microstructure of cement paste is loaded directly by underpressure, at the micrometer scale. Validation shows that creep of the cement paste must be also taken into account when good quantitative prediction is expected.*

1. Introduction

Cracks in concrete are of great concern in civil engineering worldwide. The consequence of crack formation is usually reduced structure quality or durability. This paper investigates the problem of autogenous shrinkage from the stage of concrete setting further, using experimental data accompanied by numerical simulation.

During the cement hydration, the absolute volume of cement, hydration products and water decreases. This phenomenon is called chemical shrinkage. Let us denote V_{wh} as the water consumed during the hydration, V_{ch} as the volume of hydrated cement, V_h as volume of hydrates and V_{cs} the "missing volume" of chemical shrinkage:

$$V_{wh} + V_{ch} = V_h + V_{cs}. \tag{1}$$

If the designed mix does not contain sufficient excess of water, voids necessarily appear in the structure of hardening cement paste. Water loss in this case is not caused by evaporation, but by binding into hydration products. This phenomenon is called self-desiccation and the voids correspond to chemical shrinkage V_{cs}. Additional water loss from the voids may set off additional drying shrinkage, which is not examined here. When some kinematic restrains exist in a construction, the shrinkage results in the stress initialization, exceeding several times the tensile strength of young concrete.

After mixing concrete with water, a fast reaction of tricalciumaluminate occurs, accompanied by a strong exothermic effect. This reaction results in the formation of a thin film on dispersed cement grains formed by fine ettringite crystals. As a consequence, further hydration

[1] Ing. Vít Šmilauer, Ph.D., Ing. Jiří Litoš, Czech Technical University in Prague, Faculty of Civil Engineering, Thákurova 7, Praha 6, 166 29, tel. +420 224 355 417, vit.smilauer@fsv.cvut.cz, litos@fsv.cvut.cz

is suppressed, the temperature drops - a period of incubation occurs during which the concrete mix continues to behave as a quasi-liquid. The exothermal hydration implies a rapid growth of temperature within the system. Inside, shrinkage probably occurs, manifested by the voids growth in the system.

By definition, autogenous shrinkage is combined from two different mechanisms: self-dessication shrinkage and expansion due to salts. These two mechanisms are hard to separate in practical experiments. Usually, autogenous shrinkage is measured in a closed system under sealed conditions, in isothermal environment without any external load. Possible temperature rise and dilatation may be substracted from the total, coming to pure isothermal autogenous shrinkage.

The processes of monitoring volume changes due to autogenous shrinkage is nowadays subject of considerable attention, which is also facilitated by the development of new structural materials and structures, among which there are, without doubt, increasingly implemented High Performance Concrete - HPC, High Strength Concrete - HSC and Self Compacting Concrete - SCC. There are more possibilities of limiting the respective volume changes in concrete. They range from choosing adequate cement types to suitable phase composition, various additions and admixtures or aggregate selection.

For illustration, Fig. 1 shows results of autogenous shrinkage from Portland cement with water-to-cement ratio (w/c) = 0.3 as measured in our laboratory on the device from Fig. 7. Plain cement paste, or modified with polyvinylalcohol (PVA) fibers, polypropylene (PP) fibers, or H Krystal M show remarkable differences. In these particular cases, the temperature of cement pastes rose from 20 °C to maximally 35 °C. Results after 40 h of hydration may be considered to give true autogenous shrinkage since the temperatures returned back to 20 °C. Note that the lines are parallel after 40 h, which leads to conclusion that the self-dessication mechanism is the same, only with different initial conditions.

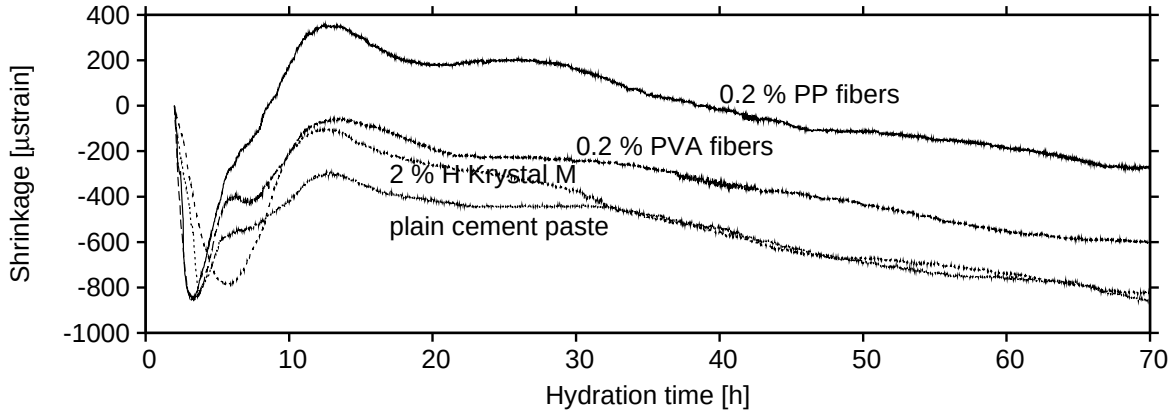

Figure 1: Experimental results of plain Portland cement paste, fiber reinforcement and crystallization admixture.

2. Capillary tension in a pore

The variation of the capillary tension is the leading mechanism of autogenous shrinkage in cement pastes [Hua 1995]. When water is consumed during the hydration, largest part of capillary

pore is emptied as the first. The meniscus in the pore causes the drop of RH in the water vapor that may be recalculated to hydrostatic water pressure via Kelvin-Laplace equation:

$$p_v - p_c = \frac{RT}{M\nu} ln(RH), \quad (Kelvin) \tag{2}$$

$$p_v - p_c = \frac{2\sigma}{r} \cos\theta, \quad (Laplace) \tag{3}$$

p_c	pressure in water,
p_v	pressure in water vapor in empty pore, often taken as zero,
R	ideal gas constant,
T	absolute temperature,
M	molar water mass,
ν	specific volume of water,
RH	relative humidity,
σ	surface tension of water,
r	radius of a pore with meniscus,
θ	moistening angle, ofter assumed zero as perfect wetting.

The validity of Kelvin-Laplace is probably above the RH of 80 %, where the capillary menisci have a radius of 5 nm [Hua 1995]. The capillary underpressure may vary from 0 to about 30 MPa, when the RH is between 100 and 80 % [Hua 1995]. The next question is, if complicated capillary network may be simplified to a cylinder-like pore, used as an assumption in Eq. (3). In reality, two principal curvatures exist on each surface of solid material.

Fig. 2 outlines two basic approaches used in the modeling of autogenous shrinkage. The first approach relies on the afore-mentioned equations while the second case uses directly data that were obtained directly from the porosimetry pressure, typically via mercury intrusion porosimetry (MIP).

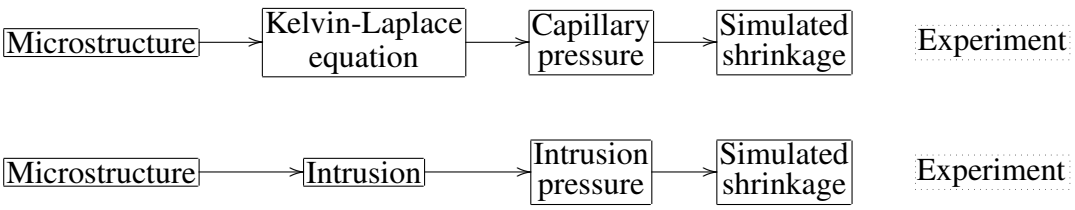

Figure 2: Approaches for the simulation of autogenous shrinkage. The top row corresponds to calculation via Kelvin-Laplace equation, bottom row is direct application of pressure as measured from porosimetry.

The second approach is based on the idea that the pressure of intruded mercury may be recalculated to that of water via the volume of chemical shrinkage. The specimen is heated up to remove the rest of capillary water and the volume V_{cs} is intruded. Due to different properties of mercury and water, the MIP pressure p_{Hg} must be recalculated to that in water p_c, that existed in the pore before the water removal:

$$p_c = \frac{\gamma_w \cos\theta_w}{\gamma_{Hg} \cos\theta_{Hg}} p_{Hg}, \tag{4}$$

where the moistening angles θ and surface tensions γ of water and mercury are tabulated. Although the MIP results are often a subject of criticism, no pore radius is calculated in this case. Instead, direct relationship volume - pressure is obtained for differently-aged specimens. The amount of empty pores may be obtained from the experiments or from a cement hydration model.

3. Cement hydration model CEMHYD3D

Any cement hydration model should reflect at least four effects: cement composition, particle size distribution (PSD), curing regime and temperature. For the purpose of mesh generation, discrete rather than continuum type of model is preferred. Cement hydration model CEMHYD3D [Bentz 2005], developed at NIST, is based on observing the development of 2D microstructure images under an electron microscope. The idea is to split up a microstructure into voxels (volume elements), typically with an edge of 1 μm. A voxel should be considered as a collection of specific phase from the neighborhood, maintaining stoichiometry of chemical reactions. The size of voxel determines the model resolution that should be small enough to capture the important undergoing processes, e.g. dissolution, transport and diffusion. Several problems occur when discretizing such continuous microstructure as that one of a cement paste. Since the resolution is limited, very fine cement particles and pores cannot be captured locally. A flowchart of the model with associated mechanical loading is shown in Fig. 3.

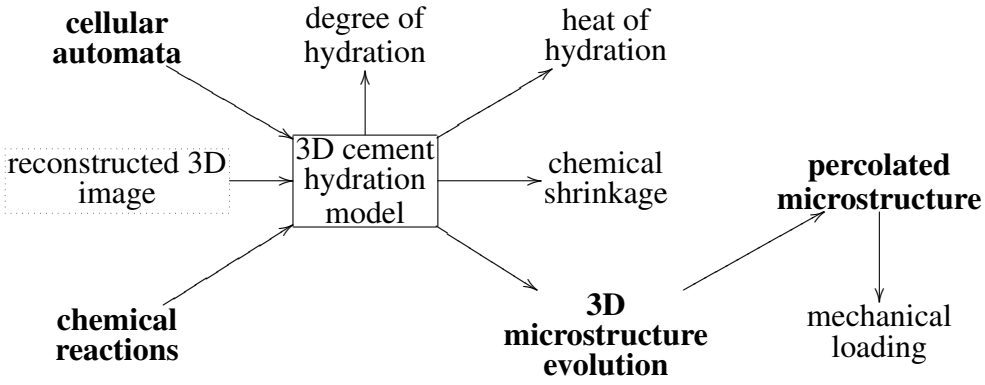

Figure 3: A flowchart of CEMHYD3D model and the calculation of mechanical response, adapted from [Bentz 2005].

The 3D microstructure, forming representative volume element (RVE), consists of chemical phases that are implemented as an ID assignment to each voxel. The rules how to handle individual voxels are called cellular automata and they define how voxels dissolve, move and what happens on their collision. Cellular automata are combined with probabilistic functions that were found effective in the description within considered model [Garboczi and Bentz 2001]. Hydration products are, with certain probabilities, formed on the grains exposed to water contact and they nucleate in the available pore space.

Initial and random 3D periodic microstructure is reconstructed with the help of autocorrelation functions and typically contains four cement clinker mineral phases and forms of calcium sulfate, all as the digital spherical particles, Fig. 4. The size of microstructure may be arbitrary,

limiting the maximal cement grain that may be placed in. Model cycles can be mapped on the time axis using a parabolic relationship [Bentz 2005].

Any model of a random system brings two sources of error: statistical fluctuation and finite size effect [Garboczi and Bentz 2001]. Statistical error emerges in any random system due to its representation, e.g. small dimensions of the cement paste. Finite size of representative cube captures only a limited piece of material that means that the sample is not statistically homogeneous. This problem may be eliminated, when representative cube is compared to the one that is considered big enough. For the *w/c* in the range from 0.25 to 0.5, the size of 100 μm is suggested [Garboczi and Bentz 2001]. Our recent results from elastic homogenization show that the reasonable size of RVE is $50 \times 50 \times 50$ μm [Šmilauer 2006].

This model of cement hydration brings also digital resolution problems. The smallest information unit is the voxel size of 1 μm, therefore any smaller size is considered only if the concentration around the neighborhood reaches that volume. This is also the case of fine capillary pores. Simulation revealed that digital resolution plays a significant role in transport issues such as diffusivity or permeability [Garboczi and Bentz 2001] but is not critical for elastic homogenization [Šmilauer 2006]. The proper size for the voxel lies probably in the range of 0.125 to 1 μm/voxel due to physical liminations [Garboczi and Bentz 2001].

The chemistry behind the hydration model will be explained on the hydration of the main mineral, $\mathrm{C_3S}$ at 20 °C. The standard cement chemistry notation will be used: C = CaO, S = $\mathrm{SiO_2}$, H = $\mathrm{H_2O}$. Numbers in parenthesis quantify the volumetric amount of the phase or the amount of colliding voxels to proceed:

$$\mathrm{C_3S}(1) + 5.3\mathrm{H}(1.34) \quad \rightarrow \quad \mathrm{C_{1.7}SH_4}(1.52) + 1.3\mathrm{CH}(0.61). \tag{5}$$

Eq. (5) means that one dissolved $\mathrm{C_3S}$ voxel may collide with one or two water voxels, producing one or two C-S-H and zero or one of CH voxel. The chemical shrinkage in this reaction is $(1.52 + 0.61)/(1 + 1.34) \sim 9\ \%$ (vol.) on average. The volumetric content in hydrating microstructure is depicted in Fig. 5. Note that label "voids" correspond to the volume of chemical shrinkage. In our case, the sealed conditions are assumed where no additional water is available therefore the voids can not be filled from external sources.

4. Autogenous modeling

The FEM will be employed for the simulation of capillary underpressure and corresponding displacements. In the simplest case, the voxel from the hydration model corresponds to one hexahedral element. Fig. 6 shows typical RVE slice. Simulation on such similar RVE yielded stiff behavior at the beginning of hydration, during homogenization of elastic properties [Šmilauer 2006]. The reason lies in the connectivity, or percolation, of solid phases. Spanning clusters are identified as connected solid voxels face-to-face and they form *percolated* RVE. On the other hand, isolated clusters are not attached to any spanning cluster and they must be disregarded in mechanical calculations, since they do not contribute to the shear stiffness. In the mesh generation, the isolated clusters are substituted by the water-filled porosity.

The node displacements in the FEM do not necessary correspond to the face-to-face connection. In certain situations, the same node displacement can not be shared by all solid neighboring

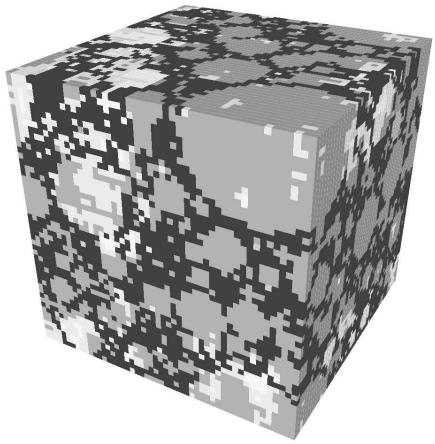

Figure 4: Example of initial RVE 50 $\times$ 50 $\times$ 50 μm, the gray levels represent clinker minerals and gypsum, black color is the water filled capillary porosity.

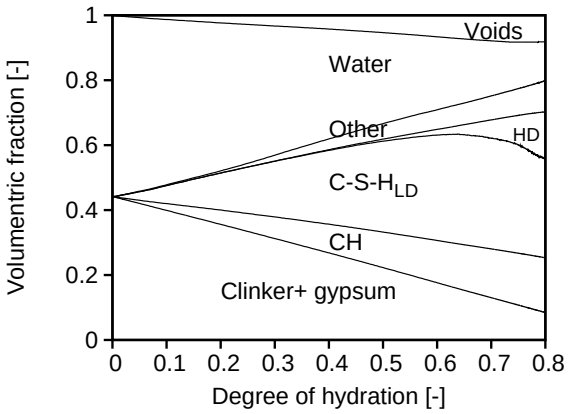

Figure 5: Volumetric content of chemical phases during hydration.

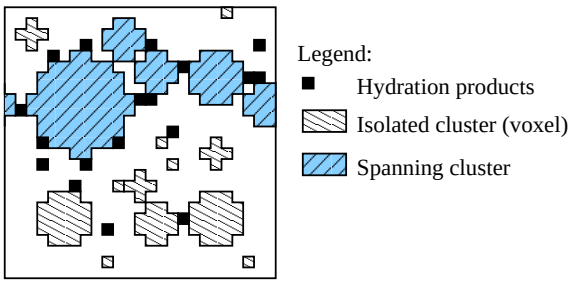

Figure 6: Typical RVE slice illustrating the connectedness.

voxels. This corresponds topologically to "sharp corners", where the stress concentration takes place. In order to avoid the refinement of the mesh, multiple node has been introduced, creating several nodes with independent displacements at one location. This situation is typical for early hydration stages, up to degree of hydration of about 0.3. Above this point, the solids in the RVE are already well connected, reducing significantly the amount of isolated clusters and sharp corners. The autogenous shrinkage is typically measured in one dimension of a specimen. The setup of such experiments is shown in Fig. 7.

The mechanical model should reflect the experimental setup. Originally, the concept of periodic unit cell (PUC) has been proposed. Such calculations have the shortcoming in accessing the stress under zero strain instead of strain without any stress. Moreover, the multiple nodes cause the discontinuous displacement field resulting in non-zero volumetric strains in the PUC. Opened capillary porosity presents even more serious problem. The PUC is a closed system, where the volumetric change is accompanied by stresses. In reality, open capillary network allows the flow of water freely from RVE, at early hydration stages.

Fig. 8 shows the final RVE, loaded in a similar manner as the experimental setup. An octant of the prism has been modeled, where the symmetry along three planes may be easily used. The bottom side has blocked vertical displacements, other two sides corresponding displacements. A stiff material is placed at the top of the RVE to average the displacements to a plane. Due to the CEMHYD3D resolution, pore network under 1 μm remains locally uncaptured.

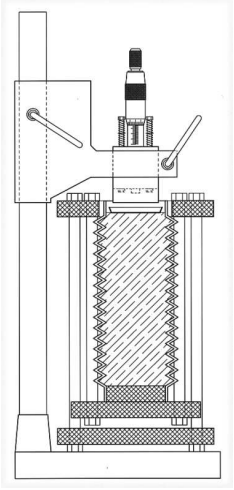

Figure 7: Typical experimental setup of the shrinkage measurement device.

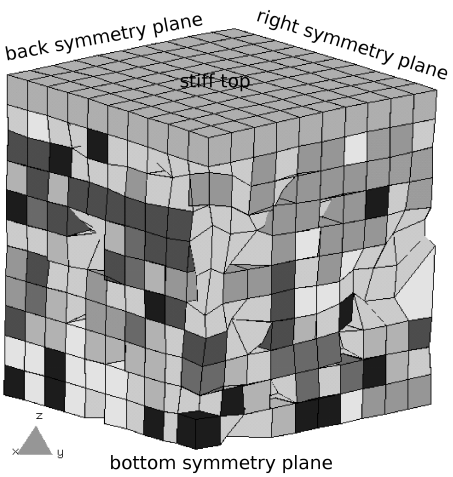

Figure 8: Example of RVE 10 $\times$ 10 $\times$ 10 μm, degree of hydration 0.2, an octant of the specimen loaded by undepressure.

The calculation procedure in the FEM package[2] has been implemented in the following manner:

- the percolated RVE is supported in three planes of symmetry, the top side allows the free movement in vertical direction,
- the water-filled porosity is loaded by a constant prescribed hydrostatic eigenstrain ϵ^{eig},
- the water vapor pressure is assumed to be zero,
- tri-linear hexahedral element represents a voxel,
- iterative conjugate gradient method solves algebraic equations from FEM.

The stresses σ in any Gauss point in the RVE are calculated from equilibrated strains ϵ^{eq}, and material stiffness matrix $\boldsymbol{C}$. The isotropic elastic constants of cement-based phases may be found in [Šmilauer 2006]. Eigenstrains ϵ^{eig} are assigned only to water-filled capillary porosity, otherwise are zero:

$$\sigma = \boldsymbol{C}(\epsilon^{eq} - \epsilon^{eig}). \tag{6}$$

Under practical simulations, $\sigma_x \doteq \sigma_y \doteq \sigma_z$ in the water filled porosity and shear components are almost zero. The pore pressure p_{cap} is calculated as the average in the water-filled capillary porosity V_w from Gauss integration points:

$$p_{cap} = \langle \sigma_x \rangle_w = \frac{1}{V_w} \int \sigma_x dV_w. \tag{7}$$

The correction of capillary pressure is necessary since also isolated clusters $V_{isolated}$ are loaded by underpressure:

$$p_{cap,corr} = p_{cap} \left(1 - \frac{V_{isolated}}{V_w} \right). \tag{8}$$

The top displacement w_{top}, corresponding to the corrected pore pressure $p_{cap,corr}$, is also calculated and averaged from the top face of the RVE, S_{face}. Average vertical strain ϵ_{sim} is

[2] SIFEL - SImple Finite ELements. Open-source package. http://cml.fsv.cvut.cz/∼sifel

calculated from the top displacement and the RVE height:

$$w_{top} = \frac{1}{S_{face}} \int w dA, \tag{9}$$

$$\epsilon_{sim} = \frac{w_{top}}{height}. \tag{10}$$

The RVE and the pore pressures changes during the hydration. The capillary stress increment is calculated is each loading step. Since linear elasticity is assumed, the history of loading allows taking a series of independent calculations and then to sum up the results:

$$w_{top,t} = \int_{t_0}^{t} w_{top,\tau} d\tau, \tag{11}$$

where $z_{top,t}$ is the top displacement at time t, t_0 is the time where the autogenous shrinkage starts. Experiments testify that this time is somewhat arbitrary and there is no general consensus about the "zero" point.

At the macroscopic level, the cement paste exhibits the behavior of viscoelastic medium. A creep function $J(t, t_0)$ is usually obtained from the creep tests at various loading times t_0. In the basic form, the creep function describes the compliance of linear viscoelastic material in terms of strains at time t due to a unit stress applied at t_0. For a homogeneous and isotropic material, two compliance functions exist, describing volumetric and deviatoric components. Preliminary results show that the deviatoric stress is at least one order lower than the volumetric one, moreover at the beginning of hydration. The reason lies in the underpressure load that has no preferential direction. Some small shear stress is induced due to imposed boundary conditions. The skeleton, or the spanning clusters in the RVE, is loaded by nearly the same stresses $\sigma_x \doteq \sigma_y \doteq \sigma_z$, therefore the constitutive equation for the vertical strain and one-dimensional creep function $J(t, t_0)$ reads:

$$\epsilon_z = (1 - 2\nu(t)) \left[J(t, t_0)\Sigma_{RVE} + \int_{t_0}^{t} J(t, \tau) \frac{d\Sigma_{RVE}(\tau)}{d\tau} d\tau \right], \tag{12}$$

where $\nu(t)$ is time-dependent Poisson's ratio, Σ_{RVE} is the macroscopic 1D stress in the RVE, t_0 is time of applied load and t is the current time. The integral of Eq. (12) is rewritten in incremental form, where the loading and $\nu(t)$ are taken from the middle of each considered interval.

The selection of material properties of porous phase is not critical, when the material contrast is high enough against the solids. The stresses of water-filled porosity are then negligible.

5. Validation

The validation of proposed algorithm will be carried out on two experiments, showing the potential of algorithms. The first experiment has been conducted by Hua *et al.* [Hua 1995], with ordinary Portland cement paste of *w/c* = 0.42. The RVE 50 $\times$ 50 $\times$ 50 μm has been reconstructured for the NIST hydration model and hydrated. Fig. 9 displays the results of predicted and measured degree of hydration. Percolated RVE entered the FFT-based elastic homogenization procedure based on periodic fields [Šmilauer 2006]. Although the FEM may handle such

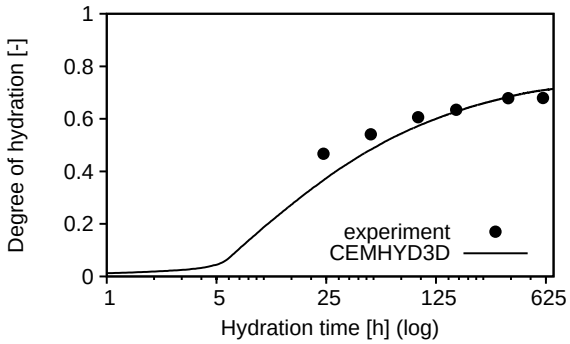

Figure 9: Simulated and predicted degree of hydration.

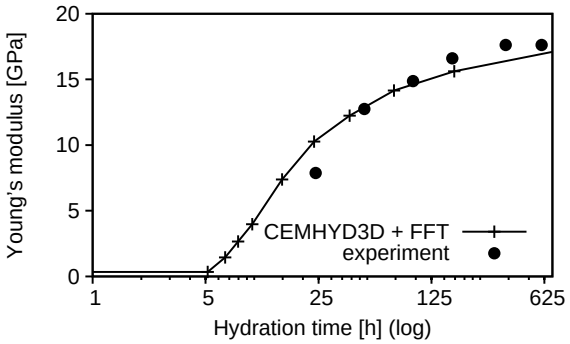

Figure 10: Evolution of Young's modulus.

kind of homogenization easily, the results are more accurate in this case. From this procedure, evolution of Young's modulus has been computed, Fig. 10.

Hua *et al.* have determined the chemical shrinkage directly from experiments. The final value of chemical shrinkage, 9.285 %, is comparable with Eq. (5). Therefore, the volume of voids under the sealed conditions, and with the reference to the degree of hydration α, is:

$$V_{cs}(t) = 0.09285\alpha. \tag{13}$$

The RVE's were loaded by a unit hydrostatic eigenstrain at the 0.05 hydration degree steps. Fig. 11 shows the macroscopic stress from such loading. Note that the macroscopic stress only in solid phases Σ_{sol} is higher than that in the RVE, Σ_{RVE}, including porosity. We assume that empty and water-filled pores do not bear any load; therefore, the difference between both stresses shows the amount of porosity. In this case, the volume of water-filled porosity at $\alpha = 0.2$ is about a half of all RVE volume, so the stress Σ_{sol} equals to applied underpressure of 1 MPa and Σ_{sol} is a half of applied underpressure.

The average displacement of the stiff lid is calculated in each load step. Fig. 12 shows the experimental MIP pressure, corrected to the water underpressure by Eq. (4). The Kelvin law, Eq. (2), allows the transition from intruded pressure to the relative humidity. For example, at α = 0.6796, the RH is 93.1 %.

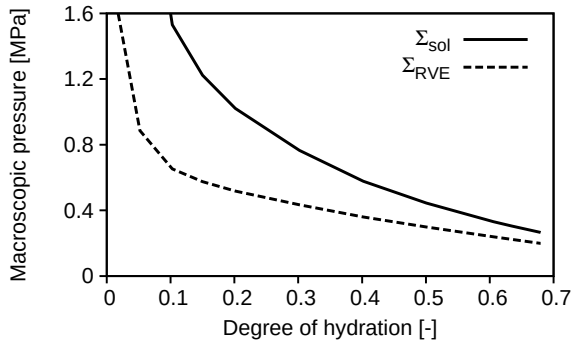

Figure 11: Macroscopic stress of solids and RVE, load 1 MPa underpressure in the capillary pores.

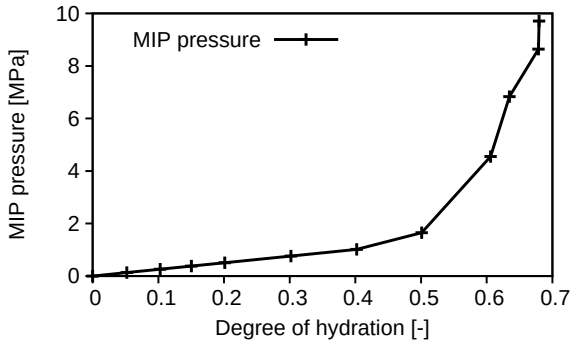

Figure 12: MIP applied pressure, corrected to water.

The creep phenomenon is ascribed to Σ_{RVE} since the stress in a creep experiment is calculated from the perpendicular sample area, including also porosity. Hua *et al.* [Hua 1995] measured also the "intrinsic" creep of loaded specimens, not including elastic effect or shrinkage. They proposed the formula of the creep part of the creep compliance function:

$$J(t,t_0) = \frac{1}{E(t_0)} + \epsilon_{cr}(t,t_0), \tag{14}$$

$$\epsilon_{cr}(t,t_0) = \epsilon_\infty(t_0)\frac{(t-t_0)^{\alpha(t_0)}}{(t-t_0)^{\alpha(t_0)} + b(t_0)}, \tag{15}$$

where $\epsilon_{\inf}(t_0)$, $\alpha(t_0)$, and $b(t_0)$ are unknown functions that must be obtained from the creep experiments for a specific sample. The load was applied at three loading times t_0, at 1, 3, 28 days. The following functions were obtained from a regression:

$$\epsilon_\infty(t_0) = 926.9 + 2707.8 \cdot 1.4667^{-t_0}, \tag{16}$$

$$\alpha(t_0) = 0.611 - 0.3024 \cdot 1.1675^{-t_0}, \tag{17}$$

$$b(t_0) = 6.6129 - 4.4624 \cdot 1.2599^{-t_0}, \tag{18}$$

where relative time from the loading, t, is in days and Eq. (15) returns μstrains. Fig. 13 displays the intrinsic creep function without the elastic response. All curves have an inflexion point.

The time discretization of Eq. (12) yielded the following procedure. The first RVE was generated at α = 0.05. Poisson's ratio and hydrostatic pressure was taken always in the middle of increment, here in α = 0.025 etc. Elastic response was calculated always at the point of interest, here at α = 0.05. The linear creep history has been considered in each analysis step.

Experimental autogenous shrinkage was measured from 24 hours, corresponding to degree of hydration of 0.4668. Fig. 14 displays the result, when the zero strain is set at α = 0.4, corresponding to 21.5 hours of hydration. In this particular case, the creep history has been neglected too. At 25 days, the elastic part takes only 14 % of total strain. Perfect agreement of simulation has been found in this case.

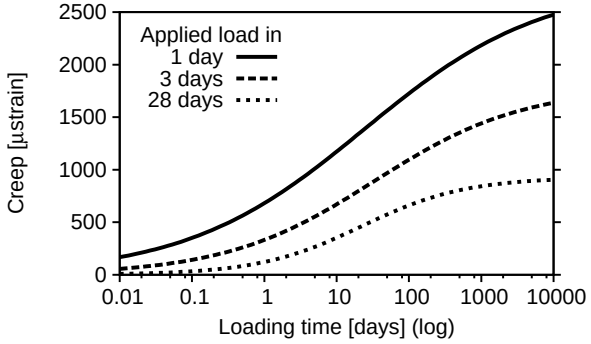

Figure 13: Intrinsic creep function of a specimen.

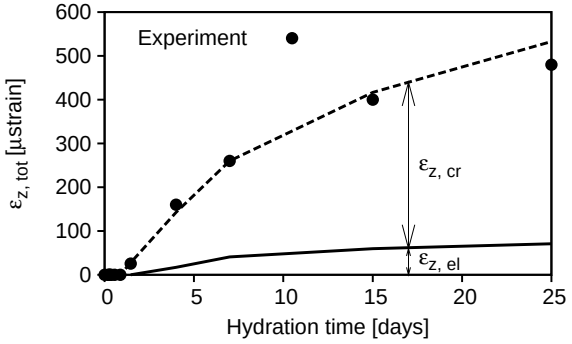

Figure 14: Total autogenous shrinkage, including creep, zeroed at the degree of hydration of 0.4 $\sim$ 21.5 h.

Second validation concerns long-time ages, based on experiments conducted by Jiang *et al.* [Jiang et al. 2005]. Prismatic sample of Portland cement paste with *w/c* = 0.3 was manufactured and stored the first day in a fog room. After 24 hours, the specimen was sealed, mounted

RH sensor and measured autogenous shrinkage. The corresponding underpressure has been estimated from our similar experiment, where the cement paste sample required around 20 MPa to fill the volume of chemical shrinkage, after a half year hydration and recalculation via Eq. (4). Assuming the same pore size during hydration, the RH may be expressed in terms of capillary underpressure, Fig. 15.

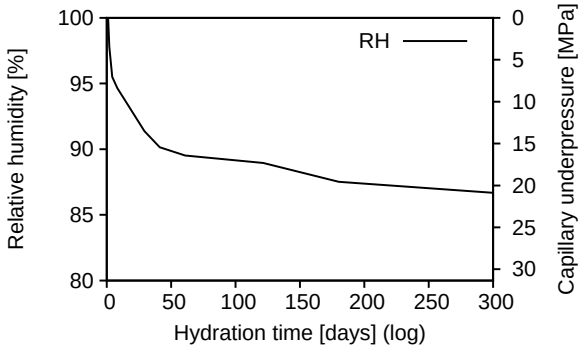

Figure 15: Measured relative humidity and assigned capillary underpressure.

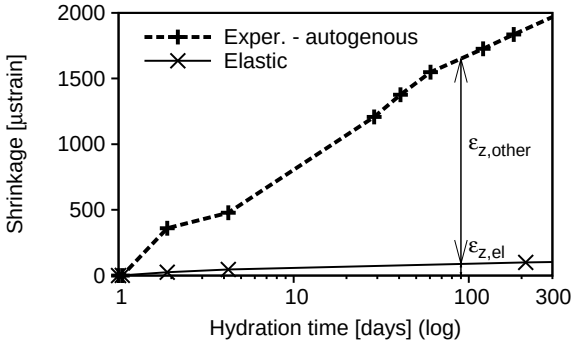

Figure 16: Autogenous shrinkage and its elastic part calculated from the hydration and FEM model.

The calculation is restricted only to elastic regime since the creep function remains unknown. Fig. 16 shows that the elastic part of autogenous shrinkage is of small importance. After 300 days, the elastic part encouters only 5 % of total shrinkage. Creep and other material processes create the most of the total shrinkage. When compared to previous experiment, the capillary underpressure is about two times higher, but acting on much smaller water-filled capillary pores. Moreover, the paste with $w/c = 0.3$ is stiffer due to large portion of unhydrated cement clinkers. This explains why the pure elastic part is smaller than in the previous case.

6. Conclusions

The capillary underpressure in the partially filled pores may be accessed directly by means of mercury intrusion porosimetry. Cement hydration model predicts the evolution of the microstructure at the resolution of 1 μm. The microstructure mesh serves as an input to FEM, loaded by the underpressure. The boundary conditions of RVE are chosen in the way of experimental setup, to simulate the length contraction. Results from macroscopic creep tests allow superposition of linear creep behavior. The validation on the $w/c = 0.42$ and 0.3 shows that the creep part creates a considerable part of autogenous shrinkage.

7. Acknowledgment

The support of project MSM 6840770003 and grant GAČR 103/04/1291 is gratefully acknowledged.

8. References

[Bentz 2005] Bentz, D.P. 2005: *CEMHYD3D: A Three-Dimensional Cement Hydration and Microstructure Development Modeling Package. Version 3.0.* NIST Building and Fire Research Laboratory, Gaithersburg, Maryland.

[Garboczi and Bentz 2001] Garboczi, E.J. & Bentz, D. P. 2001: The effect of statistical fluctuation, finite size error, and digital resolution on the phase percolation and transport properties of the NIST cement hydration model. *Cem. Concr. Res.*, vol. 31, 1501-1514.

[Hua 1995] Hua, C., Acker, P. & Ehrlacher, A. 1995: Analyses and models of the autogenous shrinkage of hardening cement paste. I. modelling at macroscopic scale. *Cem. Concr. Res.*, vol. 25, 1457-1468.

[Jiang et al. 2005] Jiang, Z., Sun, Z. & Wang, P. 2005: Autogenous relative humidity change and autogenous shrinkage of high-performance cement pastes. *Cem. Concr. Res.*, vol. 35, 1539-1545.

[Šmilauer 2006] Šmilauer, V. 2006: *Elastic properties of hydrating cement paste determined from hydration models.* PhD thesis, ČVUT in Prague, Faculty of Civil Engineering, available at http://cml.fsv.cvut.cz/ ˜smilauer.